A Story on the Wave Spectral Properties of Water Hammer

Shiblu Sarker[1*]

[1]Department of Civil, Environmental and Construction Engineering,University of Central Florida, Orlando,Florida, 32816, USA; ORCID: 0000-0001-5580-2498
[*]Corresponding author: shiblu.buet@gmail.com

Abstract

The prevention of excessive pressure build-up in pipelines requires a thorough understanding of water hammer. Seminal scholars have looked into this phenomena and come up with useful solutions using theoretical techniques. In this study, We propose a power spectral density approach on the pressure wave generated by water hammer in order to improve our understanding of the frequency-domain approach. This approach has the potential to explain some useful properties of the unsteady flow at a given section, attempting to make investigations of the dynamic characteristics of pipelines more effectively. We employ a basic pipe system to mimic the proposed approach based on the data acquired, which yields a lot of relevant physical information for pipeline construction. The proposed method is expected to be useful and efficient in gaining a better understanding of the intricate properties of unsteady flows as well as sound acoustics in a pipe system and their design.

1 Water hammer phenomena

The majority of liquids are incompressible or hardly compressible, meaning their volume does not change regardless of how much pressure is applied. This can be quite useful, such as in hydraulic cylinders, but the lack of springiness can lead to catastrophic pipe system failure, known as hydraulic transience or water hammer. To emphasize the weight of water, as we rarely carry more than a few ounces at a time. However, if one adds up all the water in a city's pipelines, or even just the pipes in a single home, it adds up to a significant amount of mass. And all of that water has a lot of momentum when it's going through a pipe. Since water is incompressible and springy, it cannot cushion the blow if the movement is abruptly stopped, for example, by quickly closing a valve. It's possible that someone is slamming concrete into the back of the valve and the pipe's walls. Instead of being absorbed, the quick change in momentum causes a pressure spike that travels through the pipe as a shockwave. When someone closes a faucet or runs the washing machine, the water hammer, slamming pipes within walls can seem a little spooky, but for large diameter pipelines, this shockwave can be heard as hammering in the walls.

So, if you have a water pipeline that is one meter in diameter and extends for a hundred kilometers, a fairly normal sized pipeline, the mass of water in the pipe is around 80 million kilos, which is a lot of kilograms. In fact, it's the equivalent of about 10 freight trains. In fact, swift closure drove those trains into a brick wall, and the pressure spike that occurs from such a sudden shift in momentum can rupture the pipe or cause major damage to other elements of the system, if someone wants to operate at the end of this pipeline in charge of closing a valve. A water hammer can be similarly harmful when a large spike in pressure ruptures a sealed container.

Another example is a 30-meter PVC pipeline with a valve on one end and a digital pressure gauge on the other to monitor pressure changes in the pipe; when the valve is closed, exciting things happen inside the pipe, and data from the pressure gauge shows that the pressure spikes to over 2000 kilopascals or about 300 PSI, which is five times the static water pressure. Due to this pressure, constructing a pipeline or pipe network Sarker (2021c) can be a little more complicated than it appears; even small spikes and pressure can pass through a system in complicated ways. A basic argument to demonstrate a few ways that engineers might reduce the risk of water hammer damage. The velocity, pipe size, time, and wave speed all affect the pressure profile of a water hammer pulse. These parameters can be modified to reduce destructive forces within the pipe system. The first is self-evident: lowering the speed at which the fluid moves through the pipe is one of the simplest methods to reduce the water's effect. Flow velocity is a function of the flow rate and the size of the pipe. When designing a pipeline, the flow rate may be fixed; as a result, one can increase pipe size to reduce velocity; a smaller pipe may be less expensive, but the flow velocity will be higher, potentially causing water hammer issues. If the pipe size is fixed, however, the flow rate can be reduced to limit the velocity, or the duration during which the change in momentum happens can be increased. Adding flywheels to pumps, for example, allows them to spin down more slowly rather than stopping. Or one can close valves more slowly to avoid issues with water hammer. The final parameter is about to adjust is the speed of sound through the fluid, that also known as wave Celerity, which describes how quickly a wave (pressure wave) can propagate through the pipe. The wave Celerity is an indirect measure of the elasticity of the system, and it can depend on compressibility of the fluid, the material of pipe and whether or not it's buried in the ground in a very rigid system. Pressure waves can reflect easily without much attenuation. For example, an anti-surge device, which contains an air bladder that can absorb some of the shock and minimize the pressure spike even further, can be added to a flexible PVC pipe sitting on the ground free to move, which can help to reduce the magnitude of the water hammer. Water towers help in surge management by allowing the free surface to move up and down, absorbing rapid changes in pressure in water distribution systems for urban areas. When water is confined, it may be as hard as concrete, and if you put two hard things together, something will eventually shatter; our job as engineers is to make sure that it isn't the costly infrastructure. Part of that entails being able to forecast pressure surges caused by water and designing devices to reduce any potential damage.

2 Water hammer wave

The conventional momentum equation Sarker (2021d,a) can be used to explain the Water hammer wave problem.

$$\sum F = \rho Q(V_f - V_i) \tag{1}$$

Where, $F =$ force, $\rho =$ density of water, $V_i =$ initial velocity of water and $V_f =$ final velocity of water. As a result, when V_f falls below V_i, a negative force is created. Within a pipeline, this negative force creates a wave of increased pressure that propagates back toward the source of the flow and goes back and forth between the source and the destination. The wave speed, also known as celerity, is a function of the theoretical wave celerity (i.e. pipe is considered to be rigid), which is given by

$$c_t = \sqrt{\frac{E_v}{\rho}} \tag{2}$$

Where, $c_t =$ theoretical wave celerity and $E_v =$ bulk modulus of elasticity of fluid. However, in reality the pipe is elastic and the velocity of a pressure wave in an elastic fluid inside an elastic pipe is given by

$$c = \frac{c_t}{\sqrt{1 + \frac{d}{t}\frac{E_v}{E}}} \tag{3}$$

Where, $d =$ pipe diameter, $t =$ thickness of pipe walls and $E =$ modulus of elasticity of pipe material. The maximum change in pressure created from water hammer in a pipeline is derived from the momentum equation 1 and results in following equation:

$$\Delta P = \rho c u_0 \tag{4}$$

Where, $\Delta P =$ change in pressure. Furthermore, When the time it takes for a valve to close is less than the pipe length divided by the wave celerity (i.e. $t = L/c$), it's called a rapid valve closing. Hence, the maximum pressure P_{max} will occur in the pipe is the original pressure within the pipe P_0 plus the change in pressure (equation 5).

$$P_{max} = P_0 + \Delta P \tag{5}$$

This pressure variation will change in cycles at times equal to $t = 2L/c$ for a rapid interruption of the flow. Over time, the pressure wave will decrease due to pipe friction and damping. In other words, the pressure wave of water at a given point within a pipe oscillate, while overall steadily decreasing as time passes. Figure 1 depicts a relatively simple pipeline system in which a control valve abruptly blocks water flow from a reservoir. From the mathematical modeling point of view, if the coordinate x runs from the reservoir through depicted pipeline of diameter d We can consider the control valve at $x = L$ as an unsteady flow source. Initially, it supplies virtually no velocity fluctuation to the pipeline under the system pressure until the time reaches 0, after that it gradually increases the velocity fluctuation until $t = t_c$ Lee et al. (2010). In general, pressure and flow velocity are independent variables in hydrodynamics, but they are dependent in linear acoustics Lee et al. (2010); Sarker (2021d,a).

$$u_t = \begin{cases} 0 : \text{when } t < 0; \\ U(t/t_c) : \text{when } 0 < t < t_c; \\ U : \quad\quad \text{when } t_c < t \end{cases} \tag{6}$$

The one-dimensional compressible fluid in the pipeline has the following continuity and momentum equations Lee et al. (2010); Reza et al. (2014).

$$\frac{\delta P_x}{\delta t} + \rho c^2 \frac{\delta u_x}{\delta x} + [u_x \frac{\delta P_x}{\delta x}] = 0 \tag{7}$$

$$\frac{\delta u_x}{\delta t} + \frac{1}{\rho}\frac{\delta P_x}{\delta x} + [u_x \frac{\delta u_x}{\delta x} + f\frac{u_x|u_x|}{2d}] = 0 \tag{8}$$

Where, f = Darcy-Weisbach friction factor Sarker (2021d,a); Lee et al. (2010) and convective terms are neglected in most engineering applications because they are so small in comparison to the other terms also neglect the friction term's effect we can simplify above equations in the form of simple wave equations as below:

$$\frac{\delta^2 P_x}{\delta t^2} = \frac{1}{c^2}\frac{\delta^2 P_x}{\delta x^2} \tag{9}$$

In this study, the Fourier transform of the pressure wave P_x was adopted and analyze to infer the instantaneous valve closure behavior.

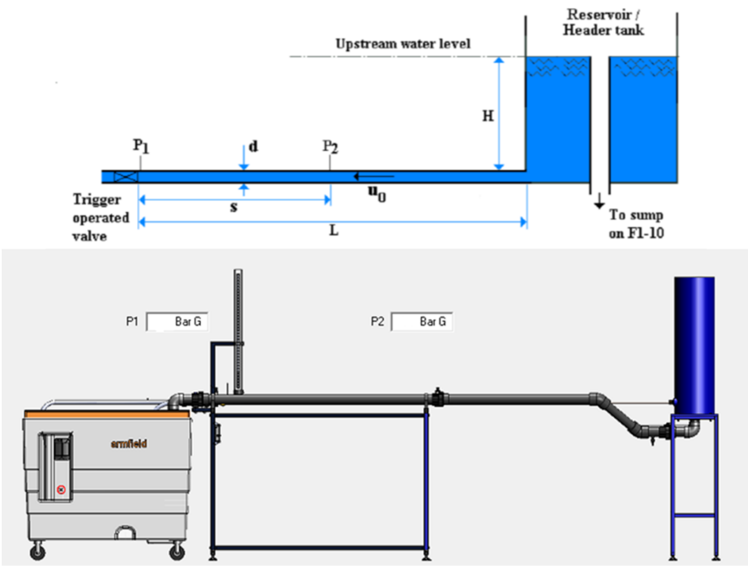

Figure 1: Schematic diagram of Water Hammer System Sarker (2021a)

3 Data collection

3.1 Experimental setup

In this section we are intended to demonstrate schematic diagram of the water hammer system to collect water hammer wave data. Figure 1 below shows the schematic diagram of the water hammer system. Figure 2-3 demonstrates the components of equipment set-up procedure for the experiment. The set up includes flow control valve in the pipe surge circuit, water hammer valve and supply control valve on hydraulic bench (see details Sarker (2021a)).

Figure 2: Laboratory Water Hammer System Sarker (2021a)

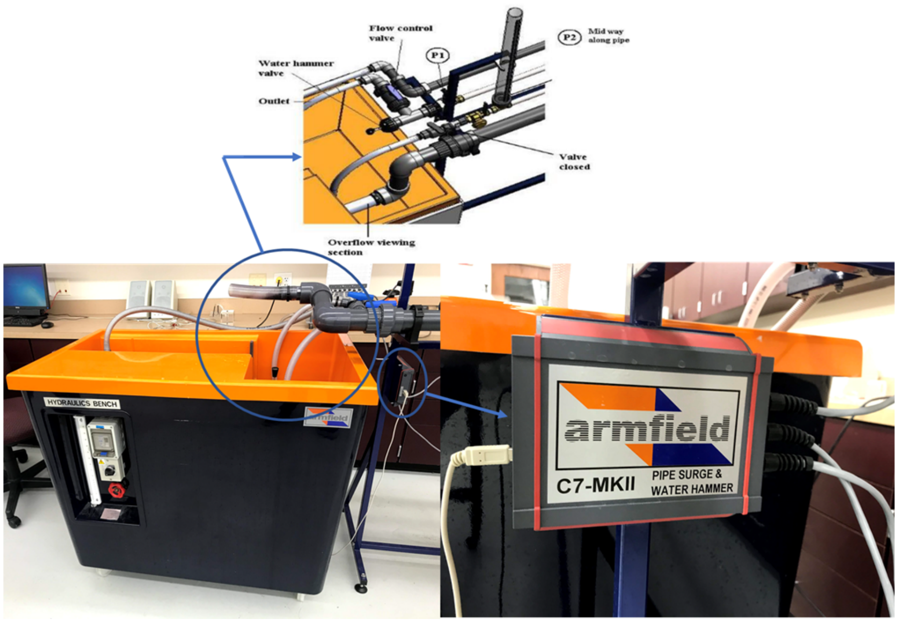

Figure 3: Components associated with the water hammer effect Sarker (2021a)

3.2 Procedure

Close the supply control valve after shutting the flow control valve on the hydraulic bench in the pipe surge circuit, then turn the black knob inwards until it latches to open the fast-acting valve on the water hammer equipment. Close the flow control valve at the end of the water hammer circuit on water hammer equipment, then turn on the pump using the switch on the hydraulic bench. Gradually open the supply control valve on the hydraulic bench and allow the header tank to fill to the level indicated by the water level in the transparent surge shaft; once the water has reached the level of the overflow inside the header tank, open the flow control valve alongside the fast-acting valve. The water will flow through the test pipe, flushing out any trapped air. Water should flow steadily through the test pipe and exit into the volumetric tank via the flexible outlet tube. If necessary adjust the supply control valve on $F1 - 10$ until a steady trickle of water returns to the sump tank via the overflow Sarker (2021a).

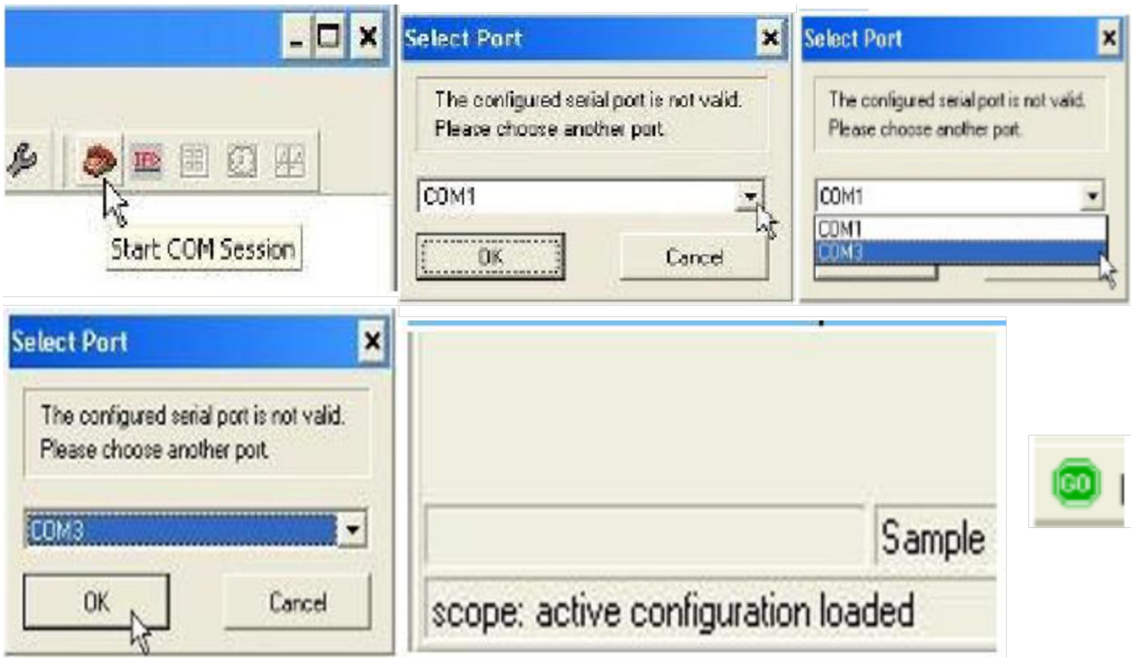

Figure 4: Data collection with C7MK11 software Sarker (2021a)

To collect pressure wave data automatically, load the Water Hammer Demonstration after loading the $C7-MK11$ software (Water hammer system) on the computer. It's time to show the welcome screen. The USB virtual serial COM port must be enabled before the software are used. To enable the port, click the Start COM Session icon at the right-hand end of the top menu bar, as shown in figure 4. The window for choosing a port will appear. Pulling down the menu reveals the available COM ports. To enable the port, select the last COM port in the list (the one with the highest number) and click OK. Check to see if the Serial Port is turned on. The virtual COM Port number followed by SE will be displayed in the bottom right hand corner if the Serial Port has been successfully activated. If the wrong Serial Port has been selected, then the number of the port will be displayed but SE will not be displayed. Display the mimic diagram and observe the readings from the two pressure sensors P1 and P2 in the water hammer circuit (indicating atmospheric pressure). The pressure changes associated with water hammer, while substantial in comparison to pipe surge pressures, only endure for fractions of a second, hence the phenomenon must be captured using a virtual oscilloscope and seen after the event, rather than being observed in real time. Allow the flow through the water hammer circuit to settle by fully opening the flow control, then fully opening the fast-acting valve. The level in the surge shaft should remain high to indicate the reservoir level. Ensure that a little amount of water is flowing back to the sump tank through the clear tube in the return pipe. Adjust the flow control valve to maintain a small flow from the overflow if necessary. The virtual oscilloscope will be enabled once the Water Hammer exercise has been loaded onto the computer, as shown by a notice in the bottom left hand corner of the screen. If the virtual oscilloscope is not automatically enabled or if the settings for the oscilloscope need to be changed, go to the Operation section, click the Go icon in the top tool bar to start logging data, then press the trigger on the fast-acting valve within approximately 2 seconds and wait until the data has been recorded and processed, then save the data.

4 Methods

4.1 The essence of the Fourier transform

The Fourier transform, which is a basic concept in understanding waves, will be discussed in this section. The major purpose of this section is to introduce it's intrinsic nature along with all of its components. To gain an idea of how this concept works, let's start with a simple example of decomposing frequencies from a sound wave, and then apply it to understanding water hammer wave characteristics.

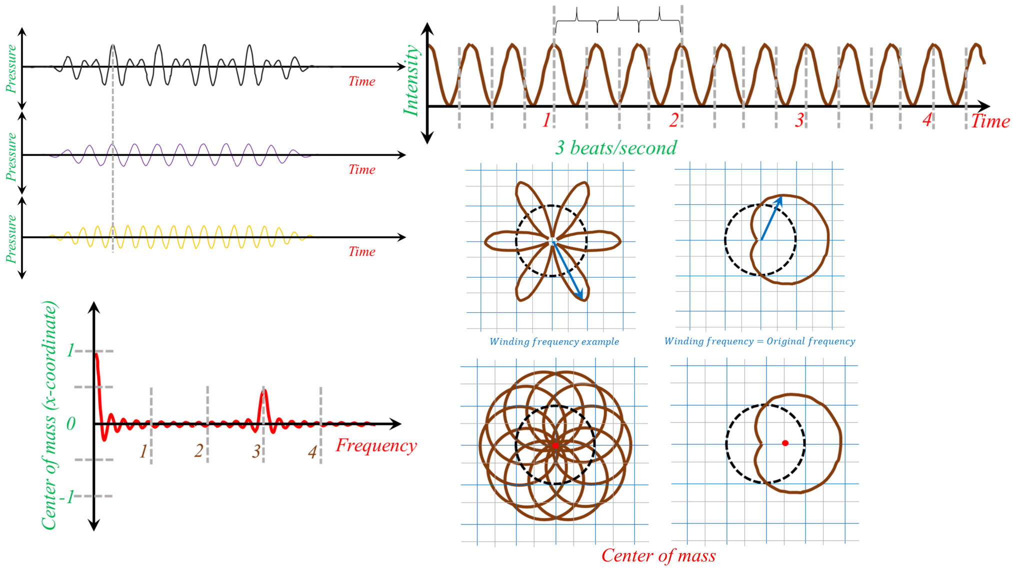

Figure 5: Illustration of the Fourier transformation and frequency decomposition (transformation of original signal from time to frequency domain) Sanderson (2018)

Figure 5 depicts a simple sound signal as a function of time (second). To put it another way, if we measured the air pressure around the source of sound as a function of time, it would oscillate up and down around its natural equilibrium, with this wave oscillating a specific number of times per second. Lower-pitched notes, on the other hand, are structured similarly to higher-pitched notes, but with fewer beats per second. When both of them are played at the same time the resulting pressure vs. time graph is going to be the sum of what it would be for each of those notes individually. At some points, the peaks match up with each other, resulting in a high pressure and at other points, they tend to cancel out. All in all, what we get is a pressure wave vs. time graph, that is not a pure sine wave but something more complicated. Similarly, if more notes are added, the wave becomes increasingly complex. Figure 5 is a mixture of two pure frequencies, which appears complicated given the small amount of information put into it, such as a microphone recording sound and displays the total cumulative air pressure at different points in time. The general strategy will be to design a mathematical machine that treats signals with a specific frequency differently than it treats other signals, which is a complicated thing to think about.

As a result, we can consider a pure finite signal with three beats per second, with the considered portion ranging from zero to 4.5 seconds (figure 5). The essential concept is to wrap this signal around a circle, or to imagine a small rotating vector whose length is equal to our signal's height at each point in time. As a result, the signal's high points correspond to a greater distance from the origin, while the signal's low points correspond to a closer proximity to the origin. We can draw it so that moving forward two seconds in time equates to one rotation around the circle, and our vector drawing this wound-up graph rotates at half a cycle every second. So, from here, we can conceive of two different frequencies: the original signal's frequency, which goes up and down three times per second, and the frequency with which we're wrapping the signal around the circle, which is half a rotation per second. In fact, we can also think of this second frequency is adjustable in such a way that we can wrap it around faster or slower.

Furthermore, the choice of this second frequency, or winding frequency, determines the appearance of the wound-up signal, and therefore, such intricate signals, which are just a type of signal that wraps the original signal around a circle, conveyed attractive physical inferences. The vertical lines are simply a means to keep track of the distance between the original signals that corresponds to a full circle rotation. When the winding frequency matches the frequency of our signal, for example, all the high points on the graph occur on the right side of the circle and all the low points occur on the left, it takes 1.5 seconds to complete one full round. To construct a precise frequency-unmixing machine, assume this signal has mass, like a metal wire, and this little dot represents the center of mass of that wire. As the frequency changes and the signal winds up differently, that center of mass wobbles around a little. When the winding frequency is the same as the frequency of our signal, all the peaks are on the right, and all the valleys are on the left, and the peaks and valleys are all spaced out around the circle in such a way that the center of mass stays close to the origin. Therefore, the center of mass is unusually far to the right. Here, to show this, we can plot that keeps track of where that center of mass is for each winding frequency. For simplicity, we can just think of only x-coordinate of the center of mass, however, it is a two-dimensional coordinate. Therefore, for zero frequency when everything is bunched up on the right, this x-coordinate is relatively high and as increasing winding frequency, and the signal balances out around the circle, the x-coordinate of that center of mass goes closer to zero. Therefore, when we have any intensity vs. time signal then we can create a wound-up version of that in some two-dimensional plane and plot the winding frequency influences the center of mass of the original signal. This insight motivates us to pursue our primary goal of frequency decomposition from original time series. This is an incredible idea that popularly known as "Fourier Transform" of the original signal.

In the actual Fourier transform, wound up signal is created by using x-coordinate and y-coordinate of the center of mass from the original time series, typically in the complex plane. This elegant process helps us to take a signal consisting of multiple frequencies and pick out what they are. This process for complex plane mathematically expressed as:

$$\hat{P}_x(\omega) = \int_{t_1}^{t_2} P_x(t)\, e^{-2\pi i \omega t} dt \tag{10}$$

Where this center of mass is a complex number, that has both a real and an imaginary part. In other words, it has two coordinates that has nice descriptions of winding and rotation. As we know from the Euler's formula that if e to some number times i, basically point out that number of units around a circle with unit radius, counterclockwise starting on the right. Therefore, to describe rotating at a rate of one cycle per second one could take the expression "$e^{2\pi i t}$", where t is the amount of time that has passed. Since, for a circle with radius 1, 2π describes the full length of its circumference. This small expression is a super-elegant way to capture the whole idea of winding a signal around a circle with a variable frequency f and this thing to do with this wound up signal is to track its center of mass. Apart from the small expression for the whole winding machine idea that we just discussed, we are intended to adopt the concept of power spectral density in the frequency domain of water hammer wave that is discussed in the subsequent section.

4.2 Roughness in the form of fractals

The concept of fractal is a beautiful notion to understand the blend of simplicity and complexity, it often appears to describe infinitely repeating patterns. However, the real concept of fractal along with the geometry associated with it is still unclear. Benoit Mandelbrot Rodriguez-Iturbe and Rinaldo (2001); Mandelbrot (1983) first introduce the concept of the fractal as well as fractal geometry. A common misconception is the fractals are shapes that are perfectly self-similar. For example, Von Koch snowflake consists of three parts, each one perfectly self-similar because someone get a completely identical copy of the original one. Similarly, the famous Sierpinski triangle consists of three smaller identical copies of itself. In fact, a basic tiny shape can sometimes be enough to make shapes that are far more complex shapes. Aside from the self-similar patterns, fractals have a much larger physical intuition. A more pragmatic motive would be a desire to describe natural systems in a way that captures roughness. In some ways, fractal geometry is best to describe the roughness of natural system due to the fact that, it is not overly idealized that natural system tends to look smooth if someone zoom in far enough. This concept overcome the needlessly idealization that neglect the finer details of the natural system as they are way beyond reality. Mandelbrot observed that the self-similar shapes give a basis for modeling the regularity in some forms of roughness. On the other hand, the common perception is that fractals only include perfectly self-similar shapes is another over-idealization, one that ironically goes against the real notion of fractal geometry and its origins. The real definition of fractals has to do with the idea of fractal dimension. There is a sense, a certain way to define the word dimension, in which the Sierpinski triangle is approximately 1.58-dimensional, that the Von Koch curve is approximately 1.26-dimensional, the coastline of Britain turns out to be around 1.21-dimensional. And in general, it is possible to have shapes whose dimension is any positive real number rather than natural numbers. In mathematics, dimension is something that usually only makes sense for natural numbers. For example, a line is 1-dimensional, a plane, that is 2-dimensional, the space that we live in, that is 3-dimensional, and so on. In fact, the formal definition of dimension in that context makes sense for counting numbers. The idea of fractal dimension is an abstract way to think. But the question is whether it turns out to be a useful construct for modeling the natural system. Definition of the fractal dimension is something which anywhere someone intends to see. It helps to start the discussion here by only looking at perfectly self-similar shapes.

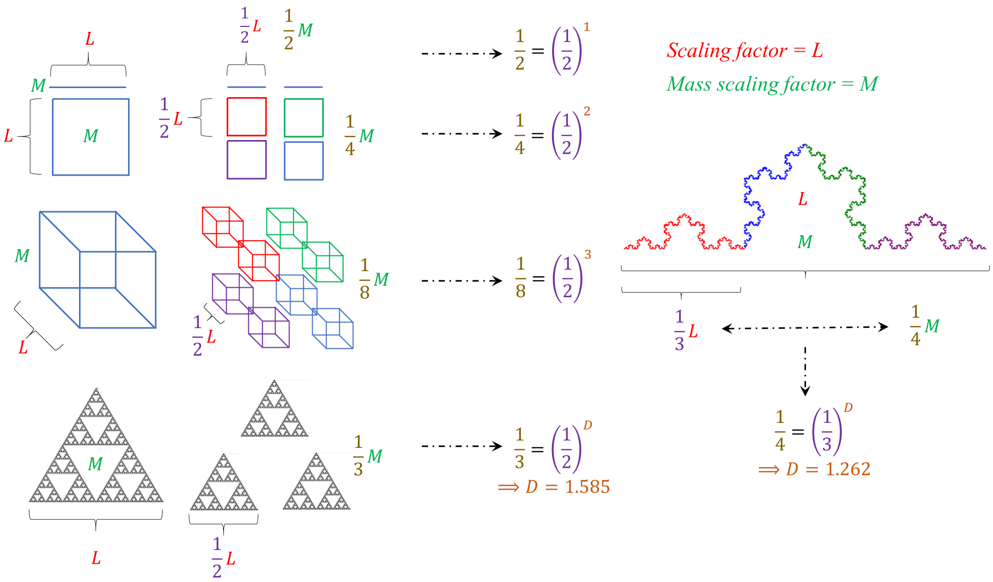

Figure 6: Fractal dimensions analogy with shape dimensions Sanderson (2017)

A line, a square, a cube, and a Sierpinski triangle are the four shapes we can begin with (figure 6), although the first three aren't even fractals, all of these shapes are self-similar. A line can now be divided into two smaller lines, each of which is a perfect copy of the original scaled down by half, a square into four smaller squares, each of which is a perfect copy of the original scaled down by half, and a cube into eight smaller cubes, each of which is a scaled down version by one-half. Besides that, the core characteristic of the Sierpinski triangle is that it is made of three smaller copies of itself, and the length of the side of one of those smaller copies is one-half the side length of the original triangle. It's fascinating to compare how we measure these scalings; we'd say the smaller line is half the length of the original line, the smaller square is one-quarter the area of the original square, and the small cube is one-eighth the volume of the original cube, but what about the smaller sierpinski triangle? To describe this concept, we can expand the concepts of length, area, and volume, which can be applied to any shape, and use the word "mass" instead of "measure" to convey a more general understanding. As a result, we can assume that each of these shapes is made of some sort of solid mass, such as a thin wire, a flat sheet, a solid cube, or a Sierpinski mesh. Then the definition can be stated as, fractal dimension is something which has a description how the mass of any shape changes when we scale them. It gives us a general approach for comparing the masses of shape with self-similarity, line by one-half, the mass is also scaled down by one-half, which we can see because it takes two copies of that smaller one to form the whole line, square by one-half, the mass is scaled down by one fourth, which we can see again by piecing together four smaller copies to get the original. Similarly, when we scale down that cube by one-half, the mass is scaled down by one eighth, or one-half cubed, because it takes eight copies of that smaller cube to rebuild the original, Sierpinski triangle by a factor of a half, it makes sense to mention that its mass is scaled down by a factor of one-third, i.e. it takes exactly three of those smaller ones to form the original. It can be notice that for the line, the square, and the cube, the factor by which the mass changed is this nice clean integer power of one half. In fact, that exponent is the dimension of each shape. In other words, it means for a shape to be, for example, two-dimensional, the "two" in two-dimensional, is that when someone scale it by some factor, its mass is scaled by that factor raised to the second power. And for a shape to be three-dimensional is that when someone scale it by some factor, the mass is scaled by the "third" power of that factor. So, if this is our conception of dimension, then the dimensionality of the Sierpinski triangle can be seen a factor of D, where the number D can be expressed in such a way that raising one half to the power of D gives us one third. In other words, that is the same as asking to 2 to the what equals 3, this quintessential type of question that logarithms are meant to answer, which is log base 2 of 3 that is about 1.58. So, in this way, this Sierpinski triangle is not 1-dimensional, instead it is 1.58-dimensional. Therefore, to describe mass of any shapes, neither length nor area the fitted another type of notion. Now we can think of another self-similar fractal, the Von Koch curve, that is composed of four smaller identical copies of itself, each of which is a copy of the original scaled down by one third. So, the scaling factor is one-third, and the mass has gone down by a factor of one-fourth. That means the fractal dimension should be some number D so that one third to the power of D is equal to one fourth, and that comes out to be around 1.26. In other words, Von Koch curve is a 1.26-dimensional shape. So, it is all just about scaling and comparing masses while scaling, everything up to this point is what someone might call "self-similarity dimension". It does a fantastic job of making the concept of fractional dimension appear sensible, but the difficulty is that it isn't a general concept. The self-similarity of the shapes, which could be built up from smaller copies of themselves, was literally relied on when we were reasoning about how the mass of a shape should change. Since we are dealing with merely geometric ones residing in an abstract space rather than tangible objects composed of stuff, this seems needlessly restrictive; after all, most two-dimensional shapes are not at all self-similar. There are a couple of ways to think about this; here is a common one.

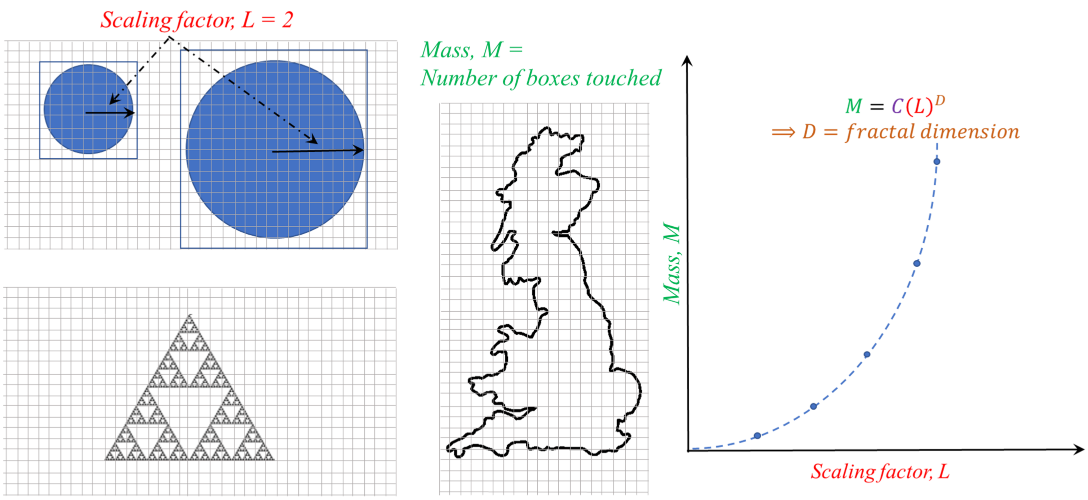

Figure 7: Generalization of fractal dimensions across scale for different shapes Sanderson (2017)

Cover the plane with the grid and highlight all the grid squares that are touching the shape. Now count how many there are. For example, we know that a disk is two-dimensional, and the number of grid squares that it touches should be proportional to its area (figure 7). A clever way to verify this empirically is to scale up that disk by some factor, like two, and count how many grid squares touch this new scaled-up version. One should find is that the number has increased approximately in proportion to the square of our scaling factor, which in this case means about four times as many boxes. In case of a much finer grid, one that more tightly captures the intent we are going for here by measuring the size of the circle, that relationship of quadrupling the number of boxes touched when you scale the disk by a factor of two should shine through more clearly. In addition, one can surprised to observe that, the plot of the scaling factor compared to the number of boxes that the scaled disk touches closely fit a perfect parabola, since the number of boxes touched is roughly proportional to the square of the scaling factor. For larger and larger scaling values, which is equivalent to just looking at a finer grid, that data is going to fit that parabola more perfectly. Now in case of the Sierpinski triangle, counting how many boxes are touching points in that shape, and if someone were to go and plot the scaling factor in this case against the number of boxes touched by the Sierpinski triangle, the data would closely fit a curve with the shape of $y = x^{1.58}$, just multiplied by some proportionality constant. Therefore, the whole reason is that we can play the same game with non-self-similar shape that still have some roughness. The most classic example we can think of the coastline of Britain. If we plop that coastline into the plane and count how many boxes are touching it, then scale it by some amount and count how many boxes are touching that new scaled version, we can see the number of boxes touching the coastline increases approximately in proportion to the scaling factor raised to the power of 1.21. The easier way is that the dimension is going to calculate from the plot of the log of the scaling factor against the log of the number of boxes touching the coastline, the relationship should look like a line, and that line should have a slope equal to the fractal dimension. Therefore, fractals are shapes, whose dimension is not an integer but instead some fractional amount and it is a quantitative way to describe the roughness of any shapes. In other words, fractals are a non-integer dimension almost entirely captures the idea of roughness. Furthermore, perfectly self-similar shapes do play an important role in fractal geometry as well as they provide us some information of this phenomenon of roughness, that persists at many different scales. Fractal dimension is not just common in nature; it appears to be the primary distinguishing factor between naturally occurring and man-made items. In this study, we are intended to use fractal dimension D as a proxy of wave roughness Sarker (2021b).

4.3 Power spectral density in the frequency domain

Power spectral density (PSD) is a frequency response measurement of the signal intensity or amplitude. In general, it provides a standard method to capture how the energy in a signal is distributed across different frequencies. The PSD $S(\omega)$ of a discrete signal $P_x(t)$ can be computed as the average magnitude of the Fourier transform squared Sarker (2021b), over a time interval and expressed as follows:

$$S(\omega) = \left| \frac{1}{2\pi} \sum_{t_1}^{t_2} P_x(t)\, e^{-i\omega t} \right|^2 = \frac{\hat{P}_x(\omega)\, \widehat{P_{x*}}(\omega)}{2\pi} \tag{11}$$

where, $\hat{P}_x(\omega)$ is the discrete Fourier transform of $g(t)$ and $\widehat{P_{x*}}(\omega)$ is its complex conjugate, and ω is the wave number Stoica et al. (2005); Stull (2012); Gardner and Robinson (1989); Sarker (2021b). We analyzed this PSD in the power-law domain across the frequency ω in the following form:

$$S(\omega)\ \frac{1}{\omega^{\beta}} \tag{12}$$

where, β is the power-law exponent of the PSD and we referred this β as proxy of roughness of wave signal, which is computed using the slope of the linear regression fitted to the estimated PSD plotted on log-log scales Pilgram and Kaplan (1998); Sarker (2021b).

4.4 Colors of noise and Hurst exponent

In physics, engineering, and many other fields, the color of noise refers to the power spectrum of a signal produced by a stochastic process i.e. noise signal. They'll sound different to human ears as audio signals, and they'll have a different texture as visuals. As a result, each application usually demands noise of a certain color. Some of the noise names have established definitions in specific areas, while others are either theoretical or poorly defined. Most of these definitions under the assumption of a signal with a power spectral density per unit of bandwidth is proportional to $1/\omega^{\beta}$ and therefore they are defined as power-law noise. White noise, for example, has a flat (i.e. $\beta = 0$), while flicker or pink noise has a $\beta = 1$, and Brownian noise has $\beta = 2$. Many time-dependent stochastic processes are known to exhibit $1/\omega^{\beta}$ noises with β between 0 and 2. Brownian motion, in particular, has a power spectral density of $4 * D_f/\omega^2$, where D_f is the diffusion coefficient Norton and Karczub (2003). In fractional Brownian motion, Hurst exponent H also show $1/\omega^{\beta}$ power spectral density with $\beta = 2H + 1$ for subdiffusive processes ($0 < H < 0.5$) and $\beta = 2$ for superdiffusive processes ($0.5 < H < 1$) Krapf et al. (2019, 2018).

The Hurst exponent is a metric for time series long-term memory. It has to do with time series autocorrelations and the pace at which they drop as the lag between pairs of values grows longer. It was established in hydrology for the purpose of calculating the optimum dam size for the Nile River's fluctuating rain and drought conditions that had been studied over a long period of time Hurst (1951). In fractal geometry discussed earlier, the generalized Hurst exponent has been denoted by H that directly related to fractal dimension, D, and is a measure of a data series' "mild" or "wild" randomness Mandelbrot and Hudson (2005). It is a term used to describe long-range dependence, which quantifies a time series' relative tendency to regress strongly to the mean or cluster in a certain direction. The value of H in the range $0.5 \sim 1$ implies a time series with long-term positive autocorrelation, whereas a value of $0 \sim 0.5$ indicates a time series with long-term flipping between high and low values in neighboring pairs. Furthermore, for self-similar time series, H is directly related to fractal dimension, D, where $1 < D < 2$, such that $D = 2 - H$.

The values of H vary between 0 and 1, with higher values indicating a smoother trend, less volatility, and less roughness Mandelbrot (1985). The Hurst exponent and fractal dimension can be chosen independently for more generic time series or multi-dimensional processes, as the Hurst exponent represents structure over asymptotically longer periods, whereas the fractal dimension represents structure over asymptotically shorter periods Gneiting and Schlather (2004).

5 Results and Discussion

The power spectral density plot was used to assess the pressure wave data collected from pressure sensors P1 and P2 Sarker (2021a,d). Figure 8a-b depicts the PSD for P1 and P2 pressure waves, respectively. Both signals, as can be shown in Figure 8, have identical characteristics. PSDs exhibit a log-log fitted slope of ~ -0.15, indicating flicker or pink noise, as opposed to merely random behavior. Furthermore, our assumption of the wave equation presented in equation 9 is supported by this pink noise property. Furthermore, the slope of PSD for P1 is slightly lower than P2, indicating a slightly higher frequency variation in the case of P2 wave than P1, which is consistent with the behavior of water hammer wave. Similarly, due to the relationship between fractal dimension (D) and Hurst exponent (H) with the slope of PSD computed, the pressure wave for P1 has a smoother trend, less volatility, and less roughness than P2. As a result of these findings, we may conclude that, in addition to natural water distribution networks Sarker et al. (2019a,b); Sarker (2021b), the proposed method may be useful in reducing pipe network Sarker (2021c) sound acoustics.

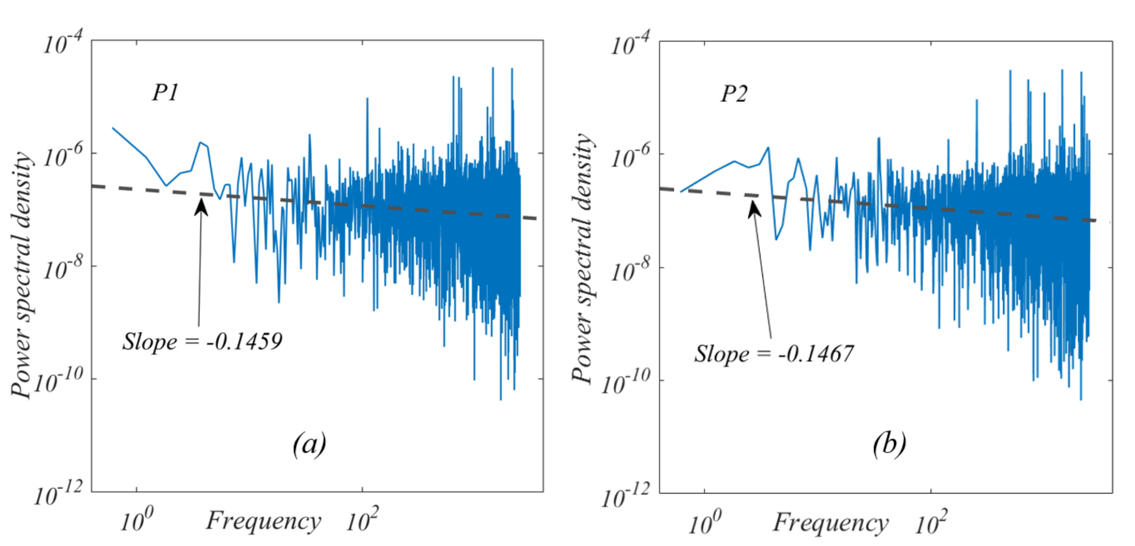

Figure 8: Power spectral density plot as a function of frequency for point P1 (a) and P2 (b), where, $\beta = Slope$ (see details in 12)

6 Concluding remarks

The main results of this study can be summarized as follows:

- We explain how the power spectral density notion and fractal nature can be used to recreate the intricate character of a water hammer wave.
- We show that the proposed method could be used in engineering design to reduce pipe network sound acoustics.

Acknowledgements

The author recognizes the explanations provided by 3blue1brown Sanderson (2018, 2017) and Practical Engineering Hillhouse (2017) on YouTube.

References

Gardner, W. A. and Robinson, E. A. (1989). Statistical Spectral Analysis—a Nonprobabilistic Theory. *Prentice-Hall, Inc., Division of Simon and Schuster One Lake Street Upper Saddle River, NJUnited States*.

Gneiting, T. and Schlather, M. (2004). Stochastic models that separate fractal dimension and the hurst effect. *SIAM review*, 46(2):269–282.

Hillhouse, G. (2017). What is Water Hammer? *Practical Engineering*.

Hurst, H. E. (1951). Long-term storage capacity of reservoirs. *Transactions of the American society of civil engineers*, 116(1):770–799.

Krapf, D., Lukat, N., Marinari, E., Metzler, R., Oshanin, G., Selhuber-Unkel, C., Squarcini, A., Stadler, L., Weiss, M., and Xu, X. (2019). Spectral content of a single non-brownian trajectory. *Physical Review X*, 9(1):011019.

Krapf, D., Marinari, E., Metzler, R., Oshanin, G., Xu, X., and Squarcini, A. (2018). Power spectral density of a single brownian trajectory: what one can and cannot learn from it. *New Journal of Physics*, 20(2):023029.

Lee, J.-S., Kim, B.-K., Lee, W.-R., and Oh, K.-Y. (2010). Analysis of water hammer in pipelines by partial fraction expansion of transfer function in frequency domain. *Journal of Mechanical Science and Technology*, 24(10):1975–1980.

Mandelbrot, B. B. (1983). The fractal geometry of nature/Revised and enlarged edition. *whf*.

Mandelbrot, B. B. (1985). Self-affine fractals and fractal dimension. *Physica scripta*, 32(4):257.

Mandelbrot, B. B. and Hudson, R. L. (2005). *The (mis) behavior of markets: a fractal view of risk, ruin, and reward*. Basic Books.

Norton, M. P. and Karczub, D. G. (2003). *Fundamentals of noise and vibration analysis for engineers*. Cambridge university press.

Pilgram, B. and Kaplan, D. T. (1998). A comparison of estimators for 1f noise. *Physica D: Nonlinear Phenomena*, 114(1-2):108–122.

Reza, A. A., Sarker, S., and Asha, S. A. (2014). An application of 1-d momentum equation to calculate discharge in tidal river: A case study on kaliganga river. *Tech. J. River Res. Inst*, 2:77–86.

Rodriguez-Iturbe, I. and Rinaldo, A. (2001). *Fractal river basins: chance and self-organization*. Cambridge University Press.

Sanderson, G. (2017). Fractals are typically not self-similar. *3Blue1Brown*.

Sanderson, G. (2018). But what is the Fourier Transform? A visual introduction. *3Blue1Brown*.

Sarker, S. (2021a). Hydraulics lab manual. *engrXiv*, DOI: https://doi.org/10.31224/osf.io/mxcvw.

Sarker, S. (2021b). Investigating topologic and geometric properties of synthetic and natural river networks under changing climatic. *UCF STARS*.

Sarker, S. (2021c). Pipe network design and analysis: An example with watercad. *engrXiv*, DOI: https://engrxiv.org/c3aky/.

Sarker, S. (2021d). A short review on computational hydraulics in the context of water resources engineering. *engrXiv*, DOI: https://engrxiv.org/t4bne/.

Sarker, S., Veremyev, A., Boginski, V., and Singh, A. (2019a). Critical nodes in river networks. *Scientific Reports*, 9(1):1–11.

Sarker, S., Veremyev, A., Boginski, V., and Singh, A. (2019b). Spectral properties of river networks. *AGUFM*, 2019:EP51C–2107.

Stoica, P., Moses, R. L., and Others (2005). Spectral analysis of signals. *Pearson Prentice Hall Upper Saddle River, NJ*.

Stull, R. B. (2012). *An introduction to boundary layer meteorology*, volume 13. Springer Science & Business Media.